Optical-strain characteristics of anisotropic polymer films fabricated from a liquid crystal diacrylate

Michael J. Escuti,[a] Darran R. Cairns, and Gregory P. Crawford[b]
Division of Engineering, Brown University, Providence, Rhode Island 02912

(Received 16 September 2003; accepted 1 December 2003)

The optomechanical characteristics of oriented polymer films made from a photopolymerizable liquid crystal diacrylate (BASF LC242) were examined, with general implications for oriented films of similar materials being used and considered for display-component applications. The birefringence of these uniaxial films before and after polymerization was determined by measuring the retardation between crossed polarizers, (resulting in $\Delta n = 0.142 \pm 0.002$ at 633 nm for the cured polymer films). Optical-strain characteristics were also determined by measuring the transmittance of the films between crossed polarizers at two wavelengths (612 and 633 nm) during the application of a monotonically increasing tensile strain. Under the conservative assumption that Poisson's ratio is constant for the relatively small strains in our experiment, we develop a strained-waveplate model to detect changes in birefringence directly from the modulation in transmittance with increasing strain. We show that strain applied along the axis of the polymer chains did not substantially affect the birefringence, and strain applied perpendicularly caused only a slight decrease (~1% decrease for 10% strain). These results highlight the robustness of fully polymerized reactive mesogen optical films to withstand the moderate strains anticipated during manufacturing processes and in-service deformation caused by bending or impact. © *2004 American Institute of Physics.*
[DOI: 10.1063/1.1643192]

I. INTRODUCTION

Control of the molecular organization of polymer films is of great importance for applications ranging from high-strength engineering materials to light-modulating passive optical elements. In particular, control over the alignment of liquid crystalline polymers is enabling the development of a wide variety of optical components for the liquid crystal display (LCD) industry.[1,2] Birefringent polymer films are integral to the performance of most LCDs, and have long served as optical compensators and retarders; however, reflective polarizers,[3] viewing-angle control films,[4] color filter arrays,[5] and scattering films[6] are also becoming prominent. As the development of flexible displays continues to be a broad and important objective within the LCD industry, display components will be subjected to potentially large strain during fabrication and use.

Several highly successful examples exist of oriented polymer optical films fabricated from liquid crystal monomers. For example, Broer and co-workers[7] fabricated broadband reflective films from mixtures of nematic and cholesteric reactive monomers, achieved by incorporating an UV absorbing dye in the monomer mixture. The gradient of light intensity through the depth of the film led to a gradient in the concentration of the chiral and nematic components (due to different polymerization rates), and therefore caused a continuously changing helical pitch throughout the film. A broadband Bragg reflection resulted. In addition, Mori and co-workers[4] have developed viewing-angle compensation films based on reactive discotic liquid crystal molecules that have an improved viewing angle for the twisted-nematic mode LCDs.

Liquid crystal (LC) monomers (often called reactive mesogens) are low molecular weight liquid crystals that can be polymerized to form high-molecular weight structures.[8,9] Most commonly, LC monomers are mono and difunctional liquid crystal acrylates,[10] epoxides,[11] and vinyl ethers.[12] Their orientation can be controlled by surfaces,[8] electric and magnetic fields,[13] shear flow, and solvents.[14,15] Sophisticated molecular architecture can thereby be permanently captured as a polymer film.

Our aim in this work is to present a basic study on the optomechanics of oriented polymer films made from a photopolymerizable liquid crystal diacrylate, and to highlight the general implications of the results for oriented films of similar materials being used for LCD components. We began by measuring the birefringence and dispersion of uniformly aligned films between glass substrates ($\leqslant 10$ μm thick). Free-standing oriented films were then prepared (~175 μm thick), and the birefringence was measured under tensile strain applied at three orientations to the nematic axis.

II. EXPERIMENT

A. Materials and processing

Throughout this work, we have used a liquid crystal diacrylate (BASF LC242[16]) in combination with the UV photosensitizer Darocur-1173 (Ciba) in the weight percent ratio 98:2, respectively. The nematic phase of LC242 persists between ~70 and 120 °C, measured using polarizing optical microscopy. No smectic phases were observed, and all of the

[a]Electronic mail: m.j.escuti@tue.nl
[b]Electronic mail: gregory_crawford@brown.edu

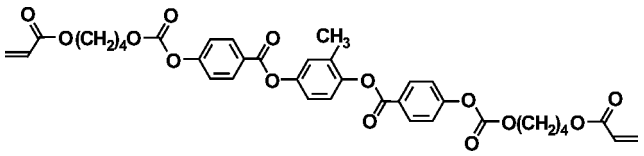

FIG. 1. Liquid crystal diacrylate LC242 ($C_{37}H_{36}O_{14}$).

films maintained their nematic order (supercooled) for several hours when brought below the crystallization temperature, a potentially useful characteristic. The chemical structure is shown in Fig. 1. Due to its rod-like structure and similarity to previously studied molecules,[8] we assume from the outset that it has a positive birefringence.

Thin cells for the initial birefringence measurements were prepared using standard glass substrates coated with rubbed polyimide (SE-2170, Nissan Chemical, ~2° pretilt angle). The cells were arranged in an antiparallel manner and partially sealed on two sides with a standard optical adhesive, while fiber spacers with 5 or 10 μm diameters were used to maintain the cell gap. Capillary action was then used to fill these cells with the prepolymer mixture at an elevated temperature (80 °C) on a hotplate. Optical measurements were taken under a variety of conditions as described in the next section.

Thicker cells for the optomechanical characterization were prepared using a 125 μm thick dogbone-shaped poly(ethylene-terephthalate) (PET) template placed between glass substrates coated with rubbed polyimide. This template was filled with the prepolymer mixture by capillary action in the same manner as the thin cells. The films were then exposed to a metal-halide UV lamp for 8 min in an ultraviolet exposure system (NuArc 26-1KS). The solid films were delaminated by separating the substrates and carefully detaching the film from the PET template. These freestanding dogbone-shaped polymer films were used for the tensile tests without further modification.

B. Birefringence calculation and model

The primary focus throughout this work is the relationship between the optical parameter of birefringence, the temperature during polymerization, and the applied tensile strain. The most natural geometry to detect this macroscopic interplay is that of the in-plane uniformly aligned birefringent film placed between crossed polarizers, with the tensile strain also applied in the in-plane direction (as discussed next). Depending on the measurement, either broadband light (from a collimated halogen lamp) or helium–neon laser probes were used for illumination.

The transmittance curve from this rudimentary spectroscopic ellipsometer can be processed along with a simple model to determine the dispersion of the birefringence. The standard expression for an *a*-plate with positive birefringence between crossed polarizers applies:

$$T=\frac{1}{2}T_0\sin^2(2\theta)\sin^2\left(\frac{\pi\Delta n d}{\lambda}\right), \tag{1}$$

where T_0 is the unpolarized irradiance incident on the first polarizer, λ is the wavelength, d is the film thickness, Δn is the birefringence, and θ is the angle between the effective optical axis of the birefringent film and the transmission axis of either polarizer (always set to 45° in our geometry). Since T is a periodic function involving a square root, the value of Δn cannot be unambiguously determined without some additional steps. We have used two methods to find the dispersion of the birefringence from the transmittance.

The first method involves a direct computation from the data as follows. From Eq. (1), the birefringence can be expressed as

$$\Delta n=(\lambda/\pi d)[m\pi\pm\sin^{-1}(\sqrt{2T/T_0})], \tag{2}$$

where m is a non-negative integer that describes the order of the solution. From basic principles of these optically transparent materials, we know that Δn is continuous across the visible spectrum. It can also be shown that the sign of the $\sin^{-1}$ function and the order m are constant between each maximum and minimum in T. Using this information, it is therefore possible to manually or computationally choose both parameters for each data point such that the ambiguity is resolved and a continuous solution of $\Delta n(\lambda)$ is found.

The second method involves an indirect solution that requires the least-squares-fit of a dispersion model to the transmittance. Since our polymer films are optically transparent throughout the visible region, the refractive index can be modeled by the first-order Sellmeier dispersion[17] relation: $n(\lambda)^2-1=a+b\lambda^2/(\lambda^2-\lambda_0^2)$, where a, b, and λ_0 are constants. Granting the standard assumptions, this can be reduced to the slightly simpler Cauchy formula: $n(\lambda)=A+B/\lambda^2$, where A and B are constants for a given material. The dispersion of our birefringent films is therefore modeled by the following equation:

$$\Delta n(\lambda)\equiv n_e(\lambda)-n_o(\lambda)\approx\Delta n_\infty+\frac{C}{\lambda^2}, \tag{3}$$

where Δn_∞ is the birefringence at long wavelengths and C is a constant. Note that the absolute values of the ordinary (n_o) and extraordinary (n_e) indices are not required to determine $\Delta n(\lambda)$. In order to calculate the dispersion of the birefringence, we combine Eq. (1) and Eq. (3) and utilize least-squares minimization to find the parameters Δn_∞ and C that give the closest fit to our transmittance data.

C. Strained *a*-plate model

In addition to standard characterization of the LC242 reactive mesogen films, we were interested in the response of such uniformly aligned films under an applied tensile strain. The geometry for this arrangement is illustrated in Fig. 2. Films with thicknesses of ~175 μm were deformed in a tensile loading configuration using a miniature tensile testing machine (Rheometrics Minimat 2000). A strain-rate (based on nominal strain) of $10^{-4}\,s^{-1}$ in uniaxial tension was used while both load and displacement were recorded. Since the miniature tensile testing machine maintained an unobstructed optical path through the sample, it was well suited for incorporation into optical experiments. Three ordered nematic

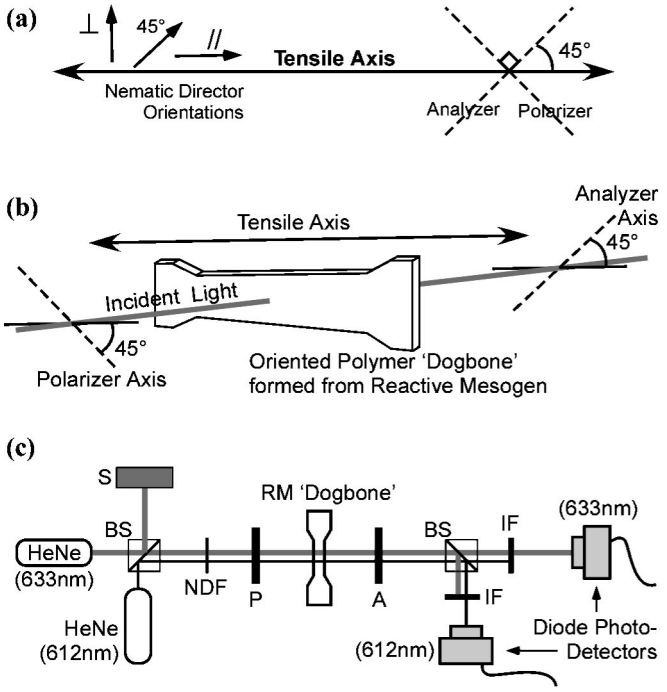

FIG. 2. Optomechanical setup: (a) nematic director and crossed polarizer orientations; (b) reactive mesogen orientation with respect to incident light and tensile axis; and (c) experimental setup, with the following abbreviations: (NDF) neutral density filter, (BS) beamsplitter, (S) beamstop, (P) polarizer, (A) analyzer, (IF) interference filter.

configurations were examined [applied strain at three angles to the mesogenic units, as in Figs. 2(a) and 2(b)]: parallel, perpendicular, and diagonal alignment of the nematic director with respect to the tensile axis. The transmittance was again modeled as a uniaxial waveplate using Eq. (1), where both the film thickness and birefringence were described as functions of the applied strain. The angle θ between the nematic director and the polarizer axes was assumed to be constant when the applied strain was parallel or perpendicular to the optical axis.

We also assumed that the film thickness d decreased linearly with applied strain, causing a noticeable modulation in the effective retardation of the film, and hence, the transmission. Since the period of this oscillation was proportional to $\lambda/\Delta nd$, the instantaneous birefringence and thickness appear as a product. For small strains the thickness is related to Poisson's ratio (v) by: $[d(\epsilon)/d_0]-1=-v\epsilon=-v[(L(\epsilon)/L_0)-1]$, where L_0 is the original gauge length, d_0 is the original film thickness, and ϵ is the nominal strain. This leads to an expression for the instantaneous thickness where the only unknown parameter is Poisson's ratio for the film:

$$d(\epsilon)=d_0[1-v\epsilon]. \tag{4}$$

Finally, the combination of Eqs. (1) and (4) leads to the general equation governing the strain dependent transmission:

$$T=\frac{1}{2}T_0\sin^2(2\theta)\sin^2\left(\frac{\pi d_0}{\lambda}\Delta n(\epsilon)(1-v\epsilon)\right). \tag{5}$$

If the birefringence does not vary substantially with strain $[\Delta n(\epsilon)=\Delta n]$, as will be shown for the parallel alignment configuration, Eq. (5) can be simplified somewhat, while no simplification is available for the perpendicular configuration:

$$T_{\parallel}=\frac{1}{2}T_0\sin^2\left(\frac{\pi\Delta nd_0}{\lambda}[1-v\epsilon]\right), \quad (\parallel \text{ case only}). \tag{6}$$

The transmission of the strained polymer film is therefore dependent on the product of two unknown parameters: $\Delta n\cdot v$, the birefringence and Poisson's ratio. At least two different wavelengths must therefore be used to uniquely determine these values. We have chosen the wavelengths 612 and 633 nm since they are conveniently available and because we observed in our original birefringence measurements of LC242 that the dispersion between these wavelengths was small enough to consider $\Delta n_{633}=\Delta n_{612}$.

The optomechanical setup is described in Fig. 2(c). Two helium–neon lasers were superimposed and normally incident on the film placed between crossed polarizers. As illustrated in Fig. 2(b), the tensile axis was placed 45° to the polarizer axes. The output from the analyzer was then split and passed through narrow-band interference filters in order to separate the two wavelengths to enable independent monitoring.

III. RESULTS AND DISCUSSION

A. Birefringence of oriented reactive mesogen films

In preparation for our main experiment studying the effects of strain on the birefringence of oriented reactive mesogen films, we began by characterizing the basic optical properties of the oriented polymer and monomer (without strain). Three aspects were important: the dispersion of the polymer birefringence, the dependence of the birefringence on polymerization temperature, and to a lesser extent, the prepolymerization birefringence of the monomer.

For these measurements, thin cells (5 and 10 μm) were prepared as described above. The transmittance of these films was then measured between crossed polarizers at various temperatures before and after polymerization using a broadband light source and a PR705 spectroradiometer (Photo Research Inc.). For example, data from two samples polymerized at different temperatures is shown in Fig. 3(a). Also shown is the best fit [of Eq. (1) combined with Eq. (3)] for each sample. The calculated birefringence (using the direct and indirect methods described above) is shown for each sample in Fig. 3(b). The sample polymerized at room temperature (23 °C) resulted in $\Delta n_{633}=0.142$, with an error of ± 0.002 determined from an ensemble of eight similarly prepared samples. The least-squares minimization resulted in $\Delta n_{\infty}=0.123$ and $C=7818\,\text{nm}^2$ as the best fit for the dispersion constants for samples polymerized at room temperature. Furthermore, the difference in the birefringence between two helium–neon laser wavelengths (633 and 612 nm) was small $(\Delta n_{633}-\Delta n_{612}=-0.001)$. The sample polymerized at elevated temperature (80 °C) resulted in a lower birefringence, caused by the decrease in the nematic order parameter of the monomer before polymerization.

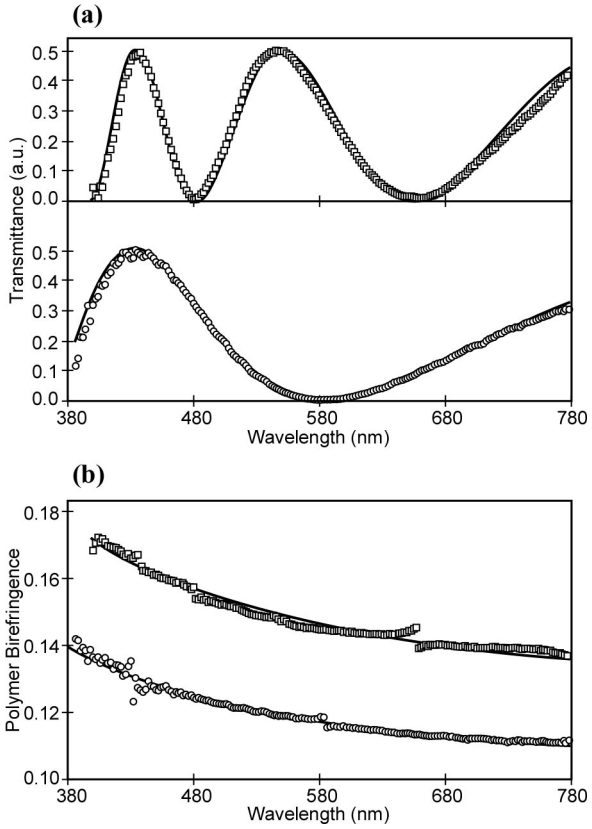

FIG. 3. Representative data for uniaxial polymer films: (a) transmittance between crossed polarizers, and (b) birefringence calculated using Eq. (2). Squares correspond to a cell of 10 μm thickness polymerized at 23 °C, and circles correspond to a cell of 5 μm thickness polymerized at 80 °C. The best fits using Eqs. (1) and (2) are shown as solid lines.

The birefringence of the aligned polymer films was measured as a function of polymerization temperature, and is shown in Fig. 4. The resulting Δn decreased monotonically, and is an example of how polymer films can be produced with controllable birefringence simply by adjusting the temperature during polymerization. The birefringence of the aligned monomer was also measured as a function of ambient temperature, plotted in the same graph in Fig. 4. For much of the temperature range, Δn for the monomer was somewhat higher than in the polymer film, and falls off more rapidly near the isotropic transition. Below ~30°, however, Δn for the polymer was higher, perhaps due to the existence of a smectic phase inducing higher order as the polymer was formed. Both curves follow the typical behavior of a low-molecular weight nematic approaching the clearing temperature. All of these results for the polymer and monomer films are consistent with dispersion characteristics of a similar mixture previously reported.[8,18]

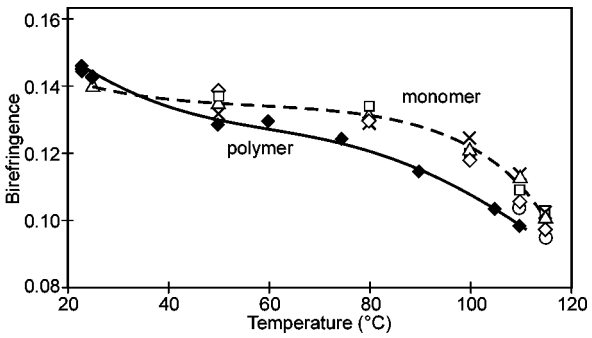

FIG. 4. Polymer: measured birefringence at 633 nm for polymer films polymerized under a variety of temperatures (solid diamonds), where the solid line is drawn to guide the eye. Monomer: also shown is measured birefringence data for monomer films at a range of ambient temperatures; results from monomer films of thicknesses of 5 μm (open diamonds, triangles, circles) and 10 μm (open squares, crosses) are shown, where the dashed line is drawn to guide the eye. Note that the abscissa denotes temperature during polymerization for the polymer, while it denotes ambient temperature for the monomer.

B. Mechanical deformation of oriented polymer films under strain

The measured Young's moduli of the thicker freestanding films were 0.81 GPa for parallel alignment, 0.55 GPa for perpendicular alignment samples, and 0.68 GPa for 45° alignment. This is consistent with Broer's findings where he measured the dynamic tensile modulus of similar monomers (between 1–2 GPa).[18] These mechanical properties resemble that of many oriented polymer structures, with a higher modulus parallel to the direction of the chains than perpendicular. The moduli of both the 45° and the isotropic films are essentially the average moduli from the other two orientations.

C. Optical response of oriented polymer films under strain

The normalized optical response of a parallel-aligned sample under tensile strain is shown in Figs. 5(a) and 5(b). The period of oscillation remains substantially constant up to mechanical failure indicating that there is little or no change in the birefringence in this alignment. This follows since the polymer chains are already aligned with the tensile axis due to the rubbed polyimide surfaces, and that no substantial director realignment occurs. Most of the films in this configuration failed at 6%–8% strain. The best-fit modeled curves are also shown in Fig. 5. The data were fit using Eq. (6) with a least-squares method with the parameters $\Delta n = 0.142$ and $d = 165\,\mu$m, resulting in a value for Poisson's ratio of $v = 0.47 \pm 0.015$. We find that there is little change in the birefringence before catastrophic failure when the film is strained parallel to the polymer chains (the optic axis).

Somewhat different behavior was revealed in the optical response for the perpendicular-alignment, as shown in Figs. 5(c) and 5(d). Most prominently, the amplitude of the modulation increased with strain. Additionally, the period of oscillation decreased with increasing strain, and the strain at break was substantially higher ($\epsilon \approx 10\%–12\%$) for most samples. Using the strained waveplate model [Eq. (5)] and the parameters $\Delta n = 0.142$ and $d = 197\,\mu$m, we found that Poisson's ratio was slightly lower than previously ($v = 0.44 \pm 0.015$) and the birefringence decreased by about ~1% ($\Delta n = 0.142 \rightarrow 0.141$) before catastrophic failure occurs. This seems reasonable, since the tensile force was in this case perpendicular to the polymer chains and was almost certainly causing local disordering of the chain links. In ef-

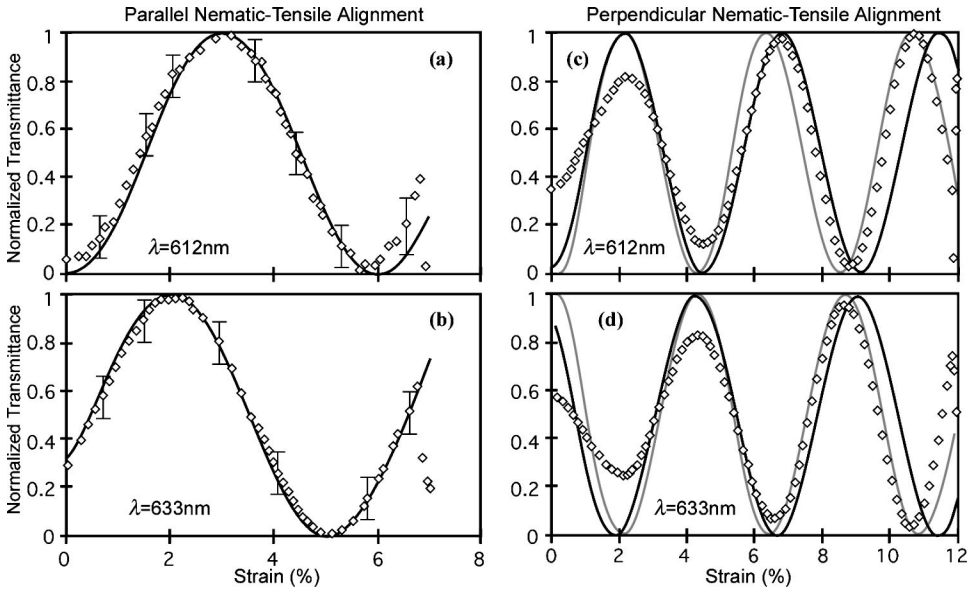

FIG. 5. Transmission characteristic of a film (165 μm thickness) with nematic axis aligned parallel to the tensile axis at (a) 612 nm and (b) 633 nm ($\diamond$) experimental data, (*black curve*) strained waveplate calculations. Transmission characteristic of a film (197 μm thickness) with nematic axis aligned perpendicular to the tensile axis at (c) 612 nm and (d) 633 nm; ($\diamond$) experimental data; (*black curve*) constant birefringence calculation, (*gray curve*) 1%-varied birefringence calculation. In all cases, the two wavelengths were recorded simultaneously.

fect, since the order parameter was decreased, the birefringence must follow. The rate of this decrease was approximately -0.0007 change in birefringence per 1% strain. It appears that the rising amplitude of the optomechanical modulation was related to a reduction of the small amount of scattering in the films as they were strained, although we have not fully characterized this.

Finally, a sample with an optical axis at 45° to the tensile axis was also examined. In this case the optical axis is parallel to the axis of the polarizer such that $\theta=0°$ and no transmission was expected unless the optical axis realigns [see Eq. (4)]. The optomechanical curve in fact remained constant, indicating no bulk realignment of the polymer chains up to 10% strain. In addition to the three ordered nematic configurations, an isotropic film was also evaluated, but also revealed no change in the optical transmission between crossed polarizers before failure.

VI. SUMMARY AND CONCLUSIONS

Birefringent films fabricated from liquid crystalline polymers are of great interest because of their many uses as passive optical films due to the ability to control their molecular organization. Characterization of anisotropic polymer films formed from the diacrylate LC242 (with surface-induced alignment) using standard optical techniques resulted in $\Delta n=0.142\pm0.002$ at 633 nm, and dispersion behavior consistent with previous reactive mesogens ($\Delta n_\infty=0.123$ and $C=7818\,\mathrm{nm}^2$). We furthermore measured the optical-strain characteristics of films oriented parallel, perpendicular, and 45° to the tensile direction and modeled the transmission in terms of a strained optical waveplate. We have shown that strain along the axis of the polymer chains does not substantially affect the birefringence, and that perpendicular strain changes the birefringence only nominally ($\sim$1% decrease for 10% strain). This points to stearic hindrance, preventing the rod-like units to acquire a higher degree of order, even when the film is stretched along the director. These results have implications on the design and fabrications limits of these materials when considering roll-to-roll manufacturing processes and in-service deformation caused by bending or impact.

ACKNOWLEDGMENTS

D.R.C. and G.P.C. acknowledge the support of Brown's NSF/MRSEC under Award No. DMR-9632524. G.P.C. acknowledges the financial support of NSF Career Award No. 9875427. M.J.E. wishes to acknowledge the support of NASA through a GSRP Fellowship.

[1] D. J. Broer, J. A. M. M. van Haaren, P. van de Witte, and C. W. M. Bastiaansen, Macromol. Symp. **154**, 1 (2000).
[2] I. Heynderickx, D. J. Broer, and T. Tervoort-Engelen, J. Mater. Sci. **27**, 4107 (1992).
[3] J. Lub, D. J. Broer, and P. van de Witte, Prog. Org. Coat. **45**, 211 (2002).
[4] H. Mori, Jpn. J. Appl. Phys., Part 1 **36**, 1068 (1997).
[5] P. van de Witte, M. Brehmer, and J. Lub, J. Mater. Chem. **9**, 2087 (1999).
[6] R. A. M. Hikmet, J. Appl. Phys. **68**, 4406 (1990).
[7] D. J. Broer, J. Lub, and G. N. Mol, Nature (London) **378**, 467 (1995).
[8] D. J. Broer and I. Heynderickx, Macromolecules **23**, 2474 (1990).
[9] D. R. Cairns, M. Sibulkin, and G. P. Crawford, Appl. Phys. Lett. **78**, 2643 (2001).
[10] D. J. Broer, J. Boven, and G. N. Mol, Makromol. Chem. **190**, 2255 (1989).
[11] D. J. Broer, J. Lub, and G. N. Mol, Macromolecules **26**, 1244 (1993).
[12] R. A. M. Hikmet, J. Lub, and J. A. Higgins, Polymer **34**, 1738 (1993).
[13] D. M. Lincoln and E. P. Douglas, Polym. Eng. Sci. **39**, 1903 (1999).
[14] D. R. Cairns, N. S. Eichenlaub, and G. P. Crawford, Mol. Cryst. Liq. Cryst. **352**, 275 (2000).
[15] H. T. A. Wilderbeek, M. G. M. van der Meer, C. W. M. Bastiaansen, and D. J. Broer, J. Phys. Chem. B **106**, 12874 (2002).
[16] F. Meyer, P. Schuhmacher, and F. Prechtl, U.S. Patent No. 6,468,444, 7 (2002).
[17] H. Y. Joo, H. J. Kim, S. J. Kim, and S. Y. Kim, Thin Solid Films **368**, 67 (2000).
[18] D. J. Broer, R. A. M. Hikmet, and G. Challa, Makromol. Chem. **190**, 3201 (1989).